Hyperfine Interact (2019) 240:95
https://doi.org/10.1007/s10751-019-1628-1

Fluorescence detection as a new diagnostics tool for electrostatic ion beam traps

Simon Lechner[1,2] · Paul Fischer[3] · Hanne Heylen[1] · Varvara Lagaki[1,3] · Franziska Maier[4] · Peter Plattner[1,5] · Marco Rosenbusch[3] · Simon Sels[1] · Frank Wienholtz[1,3] · Robert N. Wolf[3] · Wilfried Nörtershäuser[6] · Lutz Schweikhard[3] · Stephan Malbrunot-Ettenauer[1]

Published online: 20 August 2019

Abstract

In the development towards the Multi Ion Reflection Apparatus for Collinear Laser Spectroscopy (MIRACLS), an optical detection region for the observation of fluorescent light is added to an electrostatic ion beam trap (EIBT). In addition to its use for highly sensitive collinear laser spectroscopy, this fluorescence detection is introduced as a diagnostics tool for the study of the ion dynamics inside an EIBT. First measurements of collision-induced fluorescence in an EIBT demonstrate the technique's diagnostics power by tracking the evolution of an ion bunch's temporal width over its storage time inside the ion trap. Thereby, the time-focus point of the ion bunch can be determined and the influence of space-charge effects in the EIBT can be investigated. Good qualitative agreement is obtained between the measured trend of temporal widths and the simulations of the ions' trajectories in the trap. Particularly, the observation of self-bunching on the ion-bunch structure for many simultaneously stored ions is reproduced.

Keywords MIRACLS · Collinear laser spectroscopy · MR-ToF devices · EIBT · Exotic radionuclides · Collision-induced fluorescence · Ion self-bunching

PACS 29.90.+r · 37.10.Ty · 42.62.Fi

This article is part of the Topical Collection on *Proceedings of the International Conference on Hyperfine Interactions and their Applications (HYPERFINE 2019), Goa, India, 10-15 February 2019*
Edited by S. N. Mishra, P. L. Paulose and R. Palit

✉ Simon Lechner
simon.lechner@cern.ch

1 ISOLDE, CERN Experimental Physics Department, CH-1211 Geneve 23, Switzerland

2 Technische Universität Wien, Karlsplatz 13, 1040 Wien, Austria

3 Institut für Physik, Universität Greifswald, 17487 Greifswald, Germany

4 Johannes Kepler University Linz, Altenbergerstrasse 69, 4040 Linz, Austria

5 Universität Innsbruck, Innrain 52, 6020 Innsbruck, Austria

6 Technische Universität Darmstadt, Schlossgartenstr. 9, 64289 Darmstadt, Germany

1 Introduction

Collinear laser spectroscopy is a formidable tool for the exploration of the nuclear landscape in terms of ground state properties of short-lived radionuclides, such as nuclear spins, electromagnetic moments and charge radii [1, 2]. In order to access these nuclear properties by laser spectroscopy, a beam of atoms or ions is (anti-)collinearly overlapped with a narrow-band laser beam. Scanning the laser frequency around an optical transition of interest and counting the photons emitted by de-excitation from laser-excited atoms or ions reveals the hyperfine structure and the isotope shift can be determined. Fast beams at energies E of a few tens of kiloelectron volts allow one to approach the natural linewidth of an optical transition as the Doppler width $\delta\nu_{\mathrm{D}}$ is minimized according to $\delta\nu_{\mathrm{D}} \propto \delta E/\sqrt{E}$, where δE depicts the energy spread of the beam.

However, in order to access the most exotic nuclides produced with very low yields at radioactive ion beam facilities, methods with higher sensitivity have to be developed. To this end, the novel Multi Ion Reflection Apparatus for Collinear Laser Spectroscopy (MIRACLS) [3] is currently being built at ISOLDE/CERN [4]. It aims to combine the high spectral resolution of conventional collinear laser spectroscopy (based on the detection of the photons after resonant excitation) with high experimental sensitivity. This is achieved by trapping ion bunches in an electrostatic ion beam trap (EIBT) [5–8] in which the ions bounce back and forth between two electrostatic mirrors. In this way the laser-ion interaction time is increased by the number of reflections.

The EIBT used for the investigation described in this publication is very similar to multi-reflection time-of-flight (MR-ToF) mass spectrometers [9–13], applied for instance at ISOLDE for mass spectrometry of short-lived isotopes [14]. It is operated with ions of only $\approx$ 1.5 keV beam energy and serves to proof the principle of the future MIRACLS set-up for collinear laser spectroscopy designed for trapping 30-keV ions. To this end, an optical detection system is mounted in the middle of the field-free region of the EIBT in order to observe the fluorescent light.

Besides its use for collinear laser spectroscopy, fluorescence detection offers the opportunity to track the ion bunch for every passage through the optical detection region. In the following we show how this technique can be used to study the ion dynamics inside an EIBT. Specifically, collision-induced fluorescence, called residual gas afterglow in [15], has been used to examine space-charge effects and to determine the time-focus point of an ion bunch propagating inside the trap. Simulations of the evolution of the ion cloud's time structure inside the EIBT are presented and compared to experimental data obtained from fluorescence detection. These studies focus on the space-charge effect of "self-bunching", also known as "self-synchronization", in EIBTs [16–19]. Beyond its general relevance for EIBT operation with a large number of stored ions, it is crucial for the MIRACLS concept to investigate the potential influence of space-charge effects and self-bunching on collinear laser spectroscopy in an EIBT.

2 Experimental apparatus

The apparatus employed in this work is shown in Fig. 1. It is an EIBT setup originally described in [20] which has been modified for the purpose of collinear laser spectroscopy [3].

An electron-impact ion source, adapted from [21], delivers a continuous beam of singly-charged ions from stable magnesium isotopes. The Mg^+ ions are subsequently accumulated

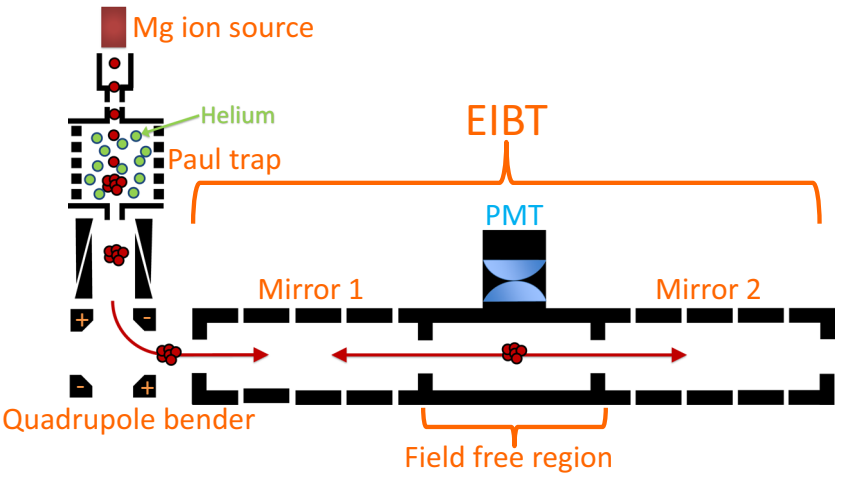

Fig. 1 Schematics of the experimental setup. A beam of Mg^+ ions is injected into a helium buffer-gas filled Paul trap from which the ions are released in bunches and captured in an electrostatic ion beam trap (EIBT). The EIBT hosts an optical detection region in its field-free region to detect fluorescence light with a photomuliplier tube (PMT). See text for details

and cooled in a helium buffer-gas filled Paul trap. They are extracted in well-defined bunches and accelerated to a transfer energy of $E_{\text{trans}} \approx 2.305\,\text{keV}$. Thereafter, the ion bunch is guided by an electrostatic quadrupole bender onto the optical axis of the EIBT. A close-up view of this EIBT is shown in Fig. 2a, depicting a central drift tube surrounded by two electrostatic mirrors. The latter consist each of a set of ring electrodes to establish the mirror potential, for instance the one shown in Fig. 2b. Capturing the ion bunch into the EIBT is achieved by the in-trap lift technique [20, 22] in which the electric potentials of the mirror electrodes are kept constant at all times. The central drift tube is switched from an initially positive bias voltage to ground potential when the ion bunch is located in the center of the tube (see Fig. 2b). Hence, the value of this "lift" potential, V_{lift}, determines the ions' kinetic energy E inside the EIBT according to $E = E_{\text{trans}} - e \cdot V_{\text{lift}}$. As long as their kinetic energy is too low to overcome the potential barrier imposed by the electrostatic mirrors, the ions are confined inside the EIBT. When the lift potential is switched back up, the ions leave the trap again. In this work, the Mg^+ ions are typically stored for a few milliseconds, while a single revolution accounts for only a few microseconds.

Similar to [23, 24], an optical detection region for fluorescence detection adapted from [25] is situated above the trap's field-free region of the central drift tube (see Fig. 1). It consists of an optical lens system, which images photons emitted by ions onto a photomuliplier.

3 Collision-induced fluorescence and tracking of the ion bunch inside an EIBT

In principle, EIBTs demand excellent vacuum quality in order to prevent the ions from colliding with residual gas particles, which affects the ion trajectories in the trap and ultimately leads to ion losses. However, there is the possibility that the collision partners undergo

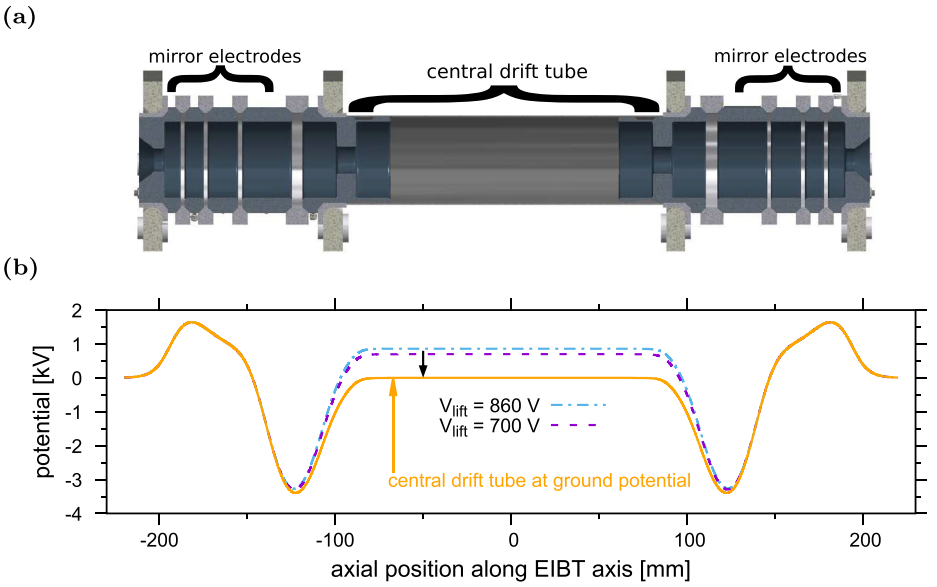

Fig. 2 **a** Schematics of the electrostatic ion beam trap (EIBT) consisting of a central drift tube and a set of electrodes forming the electrostatic mirrors. **b** Electric potential along the central axis of the EIBT used in Section 4 of this work. Prior to injection of the ions, the central drift tube is biased, e.g., to $V_{\text{lift}} = 860\,\text{V}$ (blue dashed-dotted line) or 700 V (violet dashed line). When the ions are in the field-free region of the central drift tube, it is switched to ground potential (solid orange line) as indicated by the black arrow. This results in the trapping of the ions. See text for details

inelastic collisions leading to the emission of fluorescent light. This collision-induced fluorescence can be detected in the optical detection region. Hence, every time an ion bunch passes by, the count rate of the photomultiplier increases. The temporal pattern of this photon signal reflects the time structure of the ion bunch.

Since these collisions are very rare under standard EIBT operation, the vacuum quality is purposely degraded for the following measurement. To this end, the helium flow into the Paul trap is adjusted such that the pressure in the EIBT section is increased as well. As a first application of the collision-induced fluorescence technique, the photon counts are recorded while ion bunches of stable magnesium isotopes are confined for 64 revolutions (Fig. 3). Each time an ion bunch passes the detector the number of recorded photons increases significantly above the background level.

Since a bunch passes the optical detection region twice per revolution in addition to the initial passage during capture, there are 129 pronounced peaks in Fig. 3. These are associated with $^{24}Mg^+$ ions, the most abundant magnesium isotope ($\approx$ 79%). Peaks corresponding to less abundant isotopes, $^{25}Mg^+$ and $^{26}Mg^+$, can be resolved as well. This is shown in the inset of Fig. 3. The distances between peaks associated with different magnesium isotopes increase with each revolution, due to their mass difference and corresponding difference in revolution period T, e.g. $T \approx 6.79\,\mu\text{s}$ for $^{24}Mg^+$ compared to $T \approx 6.93\,\mu\text{s}$ for $^{25}Mg^+$. In principle, this data allows the mass determination of the trapped ion species when considering the different revolution period of each isotope with respect to one magnesium isotope as a reference mass. This new fluorescence-based mass spectrometry will be

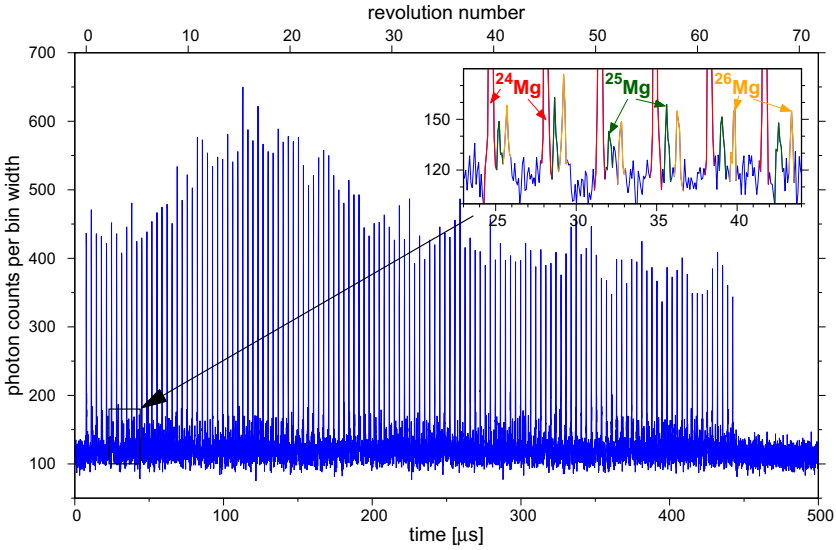

Fig. 3 Photomultiplier count rate per bin width of 40 ns as a function of time after ejection of Mg^+ ion bunches from the Paul trap, summed over about two million experimental cycles. The ion bunches are captured in the EIBT after 7.7 μs and ejected after 64 revolutions of $^{24}Mg^+$ ions which corresponds to 442.4 μs. Major signals are from fluorescence due to collisions of $^{24}Mg^+$ ions with residual-gas molecules, smaller signals are from $^{25}Mg^+$ and $^{26}Mg^+$ (see inset). The configuration of the EIBT setup is the same as described in [20]. See text for details

the topic of future work. Here, we focus our study of fluorescence detection on its capability as a diagnostics tool for the ion dynamics inside an EIBT.

In the beginning of the storage time in Fig. 3, the peak height of fluorescent light from $^{24}Mg^+$ ion collisions rises with increasing revolution number. It reaches a maximum at around 17 revolutions. Then the peak height decreases again. This behavior can be explained by Fig. 4, which characterizes the width (a), amplitude (b) and area (c) for each fluorescence peak caused by $^{24}Mg^+$ ions. Up to the 17th revolution (indicated by the blue vertical line) the peak width decreases, while the peak amplitude increases. Subsequently the behavior is reversed, with increasing width and decreasing amplitude. This is interpreted as a signature of a time focus of the ion bunch at revolution number 17. Such a time focus can for instance arise at the moment when higher energetic ions within the ion ensemble, which were initially at the temporal end of the ion bunch, overtake the slower, less energetic ions.

The almost continuously decreasing peak area shown in Fig. 4c reveals ion losses over time. These losses can arise from collisions of the ions with the residual gas. Such collisions may "kick out" ions due to the resulting transversal momentum or neutralize them by electron transfer reactions.

This first experiment illustrates that fluorescence detection in an EIBT allows one to track, in-situ and revolution by revolution, ion-bunch properties such as temporal width or relative ion number. This is complementary to the use of an image-charge detection via a pick-up electrode [16, 18, 19, 26]. Similar investigations can also be performed by ejecting the ion bunch onto an ion detector after subsequent revolution periods and evaluating the signal properties [27]. However, the measurement based on fluorescence detection only requires a single experimental cycle to record the full information for all revolutions and is not limited by the saturation-effects of, e.g. micro-channel-plate detectors.

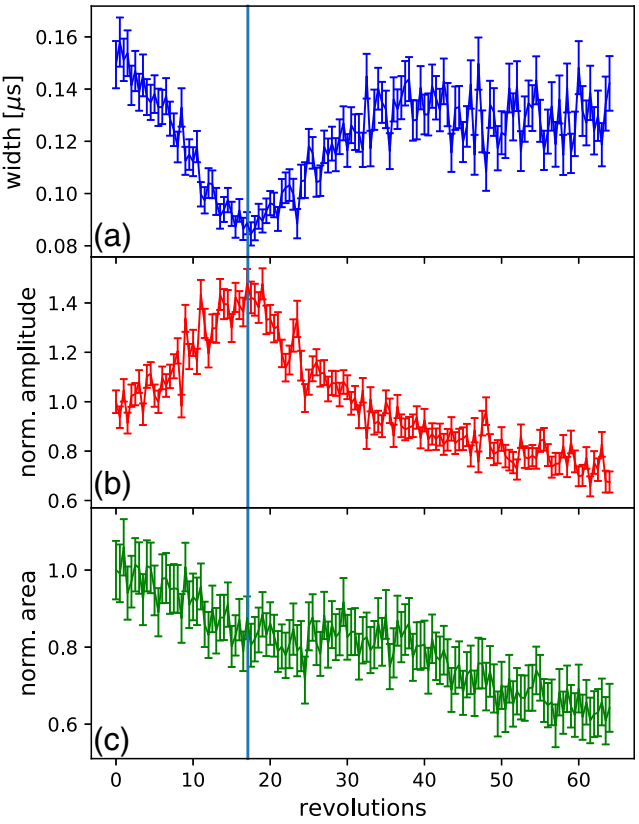

Fig. 4 Width (FWHM), amplitude and area of all peaks associated with $^{24}Mg^{+}$ ions from the data in Fig. 3 as obtained from a fit with a Lorentzian profile. $^{25}Mg^{+}$ and $^{26}Mg^{+}$ ions are included in the fit with fixed width and amplitude. The amplitude and the peak area are normalized to the number of photons in the peak corresponding to the first passage through the optical detection region. The vertical line at revolution number 17 indicates the time-focus point of the $^{24}Mg^{+}$ ion bunch. See text for details

4 Space-charge effects in an EIBT

Space-charge effects are of particular importance in the application of an EIBT as a multi-reflection time-of-flight (MR-ToF) mass separator. Indeed, large numbers of stored ions are known to disturb the otherwise superb mass resolving power of an EIBT [20, 28, 29]. Hence, understanding space-charge effects and their impact on the ion cloud in EIBTs is essential, especially when the mass separation of large ion samples is aimed for. For instance, the elimination of undesired contaminants in the beam of radioactive isotopes via MR-ToF techniques becomes increasingly important when probing exotic rare isotopes. There, additional diagnostics tools such as fluorescence detection can help1 to study and ultimately extend the limits in MR-ToF operation imposed by space-charge effects.

EIBTs used for mass spectrometry can be operated in an isochronous mode, i.e. the voltages of the trap's mirror electrodes are chosen such that within a certain energy window the revolution period T remains independent of the exact ion energy, i.e. $dT/dE = 0$. Figure 5 depicts the simulated revolution period of a $^{24}Mg^{+}$ ion bunch as a function of

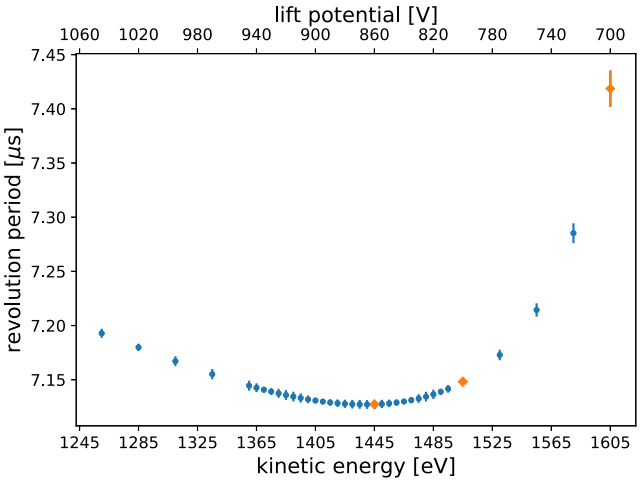

Fig. 5 Simulated revolution periods of a $^{24}Mg^{+}$ ion bunch, consisting of 1000 non-interacting ions, trapped by the mirror potentials of Fig. 2b at various ion energies. The lift potentials used to obtain these energies are indicated on the top axis. The settings marked by orange diamonds at $V_{\text{lift}} = 700$, 800 and 860 V are used for more detailed simulations that are discussed in the text

beam energy when the ions are confined in the EIBT by a potential as shown in Fig. 2b. For completeness, note that these potentials have been optimized for collinear laser spectroscopy and are not the same as those used in Section 3. As outlined above, different ion energies of the stored ions are facilitated by different lift potentials applied to the central drift tube. In Fig. 5, it can be seen that the revolution periods for lift potentials in the proximity of 860 V, corresponding to an ion energy of about 1445 eV, are very similar in a kinetic-energy range of about 10 eV. Hence, when considering ions at $E \approx 1445$ eV with energy spreads of at most a few electron volts, their individual revolution period is largely the same and the temporal ion-bunch width is consequently kept constant over time.

Contrary, for lift potentials such as below 800 V, the revolution period is noticeably influenced by the ion energy, i.e. the trap is operated in a non-isochronous mode with $dT/dE > 0$. More energetic, faster ions exhibit a longer revolution period in the EIBT compared to slower, less energetic ones. Thus, even small energy differences comparable to the typical energy spread in realistic experimental conditions lead to different revolution periods. Hence, the ion-bunch width will quickly increase with time.

However, it has been shown [16–19] that for sufficiently large ion clouds, space-charge effects counteract this bunch dispersion. This phenomenon, known as "self-bunching" or "self-synchronization", can occur for combinations of mirror potentials and ion energies where $dT/dE \geq 0$ [18] as it is the case for energies higher than $E \approx 1445$ eV (see Fig. 5). In this case, the bunch width stays roughly constant even in otherwise non-isochronous settings.

In order to investigate the importance of self-bunching in the present setup, SIMION [30] simulations of ion trajectories inside the EIBT are carried out, which follow closely the procedure described in [31]. An ion bunch is thermalized in the Paul trap and then transferred into the EIBT. The storage in the EIBT over typically 300 revolutions is simulated separately at the highest computationally feasible geometrical resolution [31]. The mirror potentials, as shown in Fig. 2b, have previously been optimized for a lift voltage of $V_{\text{lift}} = 860$ V, i.e.

ion energies of 1445 eV, but are kept identical for all simulations. As the observable of interest, the temporal bunch width is evaluated in the middle of the EIBT's field-free region for every passage.

First, simulations of 1000 non-interacting $^{24}Mg^{+}$ ions are carried out for different lift potentials and hence, different ion energies. The resulting temporal width of the ion bunch is shown in Fig. 6a. For ion energies of 1445 eV, the ion-bunch width (blue line in Fig. 6a) remains constant over the entire storage time. Thus, despite an energy spread of $\delta E = 2.36$ eV (FWHM), the EIBT operates in an isochronous mode as expected from Fig. 5. On the other hand, the bunch width increases linearly for ion energies above 1445 eV. Far away from the isochronous mode, as for $V_{\text{lift}} = 700$ V ($E \approx 1605$ eV), the ion ensemble will quickly de-bunch after a few tens of revolutions as discussed above.

In a second set of simulations, Coulomb interactions between ions as implemented in SIMION's charge repulsion method [32] are used to study the effect of space charge on the bunch width (see Fig. 6b). Already for 100 ions this is computationally expensive. To obtain results for larger ion clouds without increasing the computing time, a charge multiplication factor is applied to the Coulomb interaction between the ions [33]. When using a charge multiplication factor of 10 for example, each ion acts as a sub-bunch of 10 ions. This method may lack some degree of accuracy since the electric field does not reflect the ions' cloud charge density. However, we expect that it leads to a qualitative understanding of space-charge effects at play in the EIBT in a time efficient way. The consistency of the method is benchmarked by comparing a simulated ion cloud of 250 interacting ions to an ensemble of 100 ions, interacting with a charge multiplication factor of 2.5. In this particular case, the results on the ion-bunch width agree within statistical uncertainties. Note that the Coulomb interaction between the ions is only considered while the ions are trapped inside the EIBT to clearly isolate the space-charge effects from those occurring in the Paul trap or during ion transfer. Thus, for one fixed lift potential the initial ion distribution inside the EIBT is identical and all differences in the ion cloud's temporal width are exclusively due to different multiplication factors in the Coulomb interaction.

Figure 6b displays the results of simulations which include Coulomb interactions for a lift potential of $V_{\text{lift}} = 700$ V ($E \approx 1605$ eV). This configuration normally leads to a sizable dispersion and hence a rapid increase in the bunch width with revolution number. For 100 trapped ions, the difference in the bunch width for non-interacting and interacting ions is minimal and the slope of bunch width as a function of revolution number is quite similar. However, increasing the charge multiplication factor to resemble larger ion clouds has significant consequences: The increase in bunch width is considerably slower since Coulomb repulsion counteracts this de-bunching. This happens already for charge multiplication factors of 10 and 20, corresponding to 1000 and 2000 ions, respectively. For a charge multiplication factors of 40 and 100 the bunch width is practically constant as in the isochronous mode, indicating the effect of self-bunching.

Motivated by the results of these simulations, measurements of collision-induced fluorescence are performed similarly to those in Section 3 for different numbers of ions simultaneously stored in the EIBT. To this end, the loading time of the Paul trap is varied. However, we do not have a reliable estimate of the absolute ion number. For these measurements, nitrogen gas is directly leaked into the EIBT's vacuum chamber. The lift potential is set to 700 V, to have considerable ion bunch dispersion and a direct comparison to the respective simulation in Fig. 6b. Fluorescence signals at different revolution numbers (0, 40 and 80) of $^{24}Mg^{+}$ ions are presented in Fig. 7 for two different Paul trap loading times, 50 μs and 800 μs, respectively. The latter leads to ion clouds with significantly larger ion

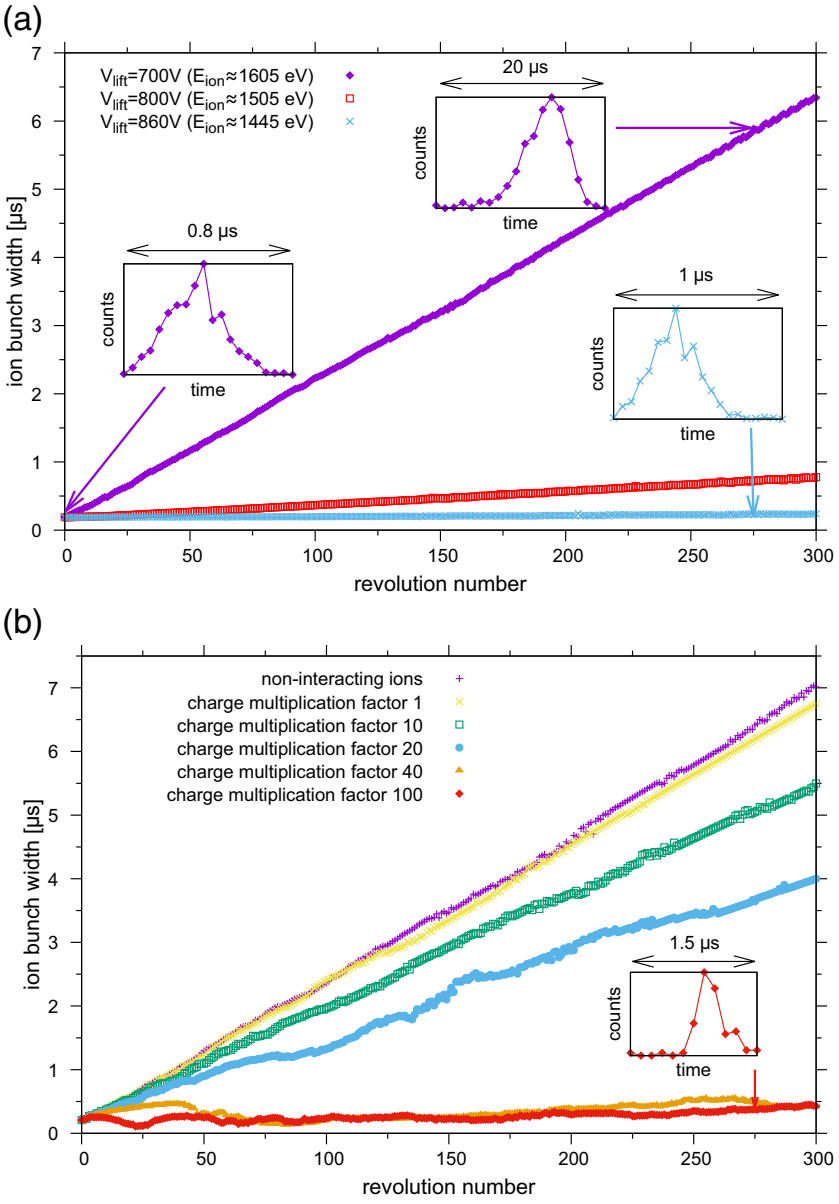

Fig. 6 Simulated temporal widths of $^{24}Mg^{+}$ ion bunches (FWHM) in the middle of the EIBT as a function of revolution number. **a** illustrates the evolution of the bunch width for different lift voltages, and thus ion energies, for 1000 ions neglecting Coulomb interactions between the individual ions. In **b**, the Coulomb interactions between 100 ions with various charge multiplication factors are considered. Here, the lift voltage is fixed to 700 V, resulting in a mean ion energy of $E \approx 1605$ eV. Within **a** and **b**, respectively, the ions are processed starting always from the same initial ion cloud as it is extracted from the Paul trap. Insets show the detailed time structure of the ion bunch at selected revolution numbers. See text for details

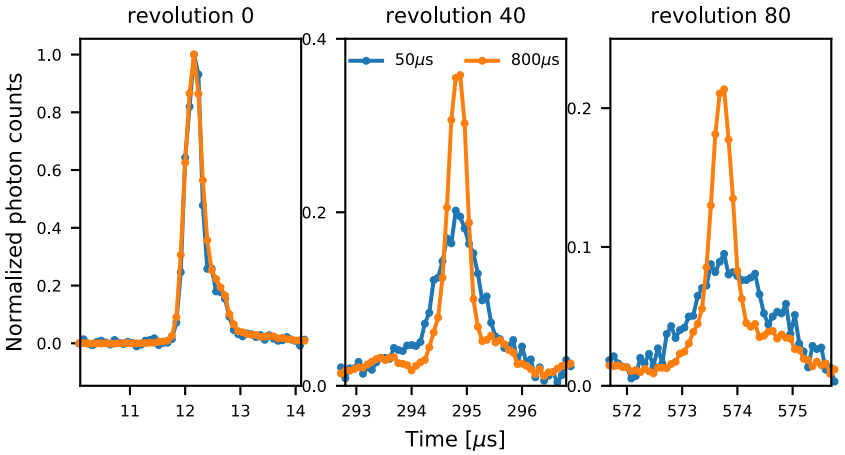

Fig. 7 Experimental time-of-flight signals at revolution numbers 0, 40 and 80 for loading times of 50 and 800 μs into the Paul trap and $V_{\text{lift}} = 700$ V. The displayed collision-induced fluorescence rate is normalized and background subtracted. The peaks are associated with $^{24}Mg^{+}$ ions, although $^{25}Mg^{+}$ and $^{26}Mg^{+}$ ions can be seen in the tail to the right at revolution 0

Table 1 Measured temporal widths of fluorescence signals (FWHM) from $^{24}Mg^{+}$ ion bunches stored inside the EIBT (for $V_{\text{lift}} = 700$ V) at different revolution numbers and Paul trap loading times

	Temporal width [μs]		
Loading time [μs]	Revolution 0	Revolution 40	Revolution 80
25	0.311(10)	0.90(6)	1.30(18)
50	0.305(9)	0.84(4)	1.34(15)
100	0.316(9)	0.70(3)	1.08(8)
250	0.314(8)	0.46(1)	0.50(2)
800	0.336(8)	0.35(1)	0.40(1)

numbers. At revolution 0, the normalized and background-subtracted peaks are close to identical for both loading times. At revolution 40, however, an ion bunch with less ions shows already clear signs of dispersion, getting even more significant at revolution number 80. On the other hand, the width of the fluorescence peaks corresponding to 800 μs of loading time remains almost constant over revolution number.

For a more quantitative analysis, the temporal signal widths, obtained by fitting the peaks in Fig. 7 with a Lorentzian profile, are listed in Table 1, along with the widths for 25, 100 and 250 μs loading time. The width at revolution 0 is similar for all loading times, except for 800 μs. Most probably, the small difference arises from space-charge effects in the Paul trap. For short loading times, i.e. small ion numbers, the bunch width increases with higher revolution number as expected from the simulations (Fig. 6b). According to the data, space-charge effects are insignificant for loading times of less than 50 μs. For longer loading times this dispersion is more and more reduced until the beam width becomes (almost) constant, i.e. independent of the revolution number. This is the case for 800 μs loading time.

This qualitative agreement of the experimental data with the simulations suggests that the underlying EIBT mechanism at play is indeed self-bunching due to space-charge effects. This analysis underlines the strength and versatility of the fluorescence-based detection.

5 Conclusion and outlook

First measurements using collision-induced fluorescence demonstrate that photo detection offers an excellent diagnostics tool for studies in an electrostatic ion beam trap (EIBT). Among others, it allows the characterization of ion losses as well as the determination of the ion-bunch width and of the ions' time-focus point. These are all crucial parameters in the study of space-charge effects such as self-bunching. The qualitative agreement between simulations of ion trajectories and the data from fluorescence detection shows that space charge has a sizable influence on the time structure of the ion bunch. Upcoming investigations will include quantitative evaluations of the ion number within an ion bunch as well as of various aspects of the photon detection efficiency during the ions' passage through the optical detection region.

However, collisions of ions with residual gas particles lead to undesired ion losses and even with purposely degraded vacuum quality the fluorescence efficiency remains low. Thus, laser-induced excitation will be explored to overcome these disadvantages.

The combined approach of fluorescence detection and simulation of ion trajectories will play an important role in the development and optimization of the Multi Ion Reflection Apparatus for Collinear Laser Spectroscopy (MIRACLS). Although MIRACLS is aiming for the study of a few stored ions of rare radionuclides, for which space-charge effects are expected to be negligible, an accurate understanding of the space-charge limits will be crucial. For instance, "contaminant" ions have to be taken into account as well as reference measurements with stable high-yield isotopes. In this regard, these future studies at MIRACLS are similar to the investigations when Paul traps were first introduced for more sensitive collinear laser spectroscopy [34, 35] and space-charge limits for the technique had to be established.

Beyond MIRACLS, fluorescence detection offers additional opportunities to probe and understand the ion dynamics in EIBT devices when used as multi-reflection time-of-flight (MR-ToF) mass separators. Here, the so-called "peak coalescence" [20, 36] instead of ion separation in time-of-flight can pose a major challenge. The extension of the present studies can help to advance the technology of MR-ToF mass separation for larger ion samples, which will be beneficial with respect to delivering contamination-free radioactive ion beams to experiments. In addition, fluorescence detection may also be applicable to MR-ToF mass spectrometry.

Acknowledgements Open access funding provided by TU Wien (TUW). The research leading to these results has received funding from the European Research Council (ERC) under the European Unions Horizon 2020 research and innovation programme under grant agreement No 679038. P.F. acknowledges support by the German Ministry for Education and Research (BMBF, 05P15HGCIA). The authors would like to thank S. Sailer and L. Bartels for their earlier contributions to MIRACLS. We are grateful for support form CERN, ISOLDE, and MPI K Heidelberg.

References

1. Blaum, K., Dilling, J., Nörtershäuser, W.: Precision atomic physics techniques for nuclear physics with radioactive beams. Phys. Scr. **T152**, 014,017 (2013). https://doi.org/10.1088/0031-8949/2013/T152/014017. https://stacks.iop.org/PhysScr/T152/014017
2. Campbell, P., Moore, I., Pearson, M.: Laser spectroscopy for nuclear structure physics. Progress Particle Nucl. Phys. **86**, 127–180 (2016). https://doi.org/10.1016/j.ppnp.2015.09.003. http://www.sciencedirect.com/science/article/pii/S0146641015000915
3. Sels, S., Fischer, P., Heylen, H., Lagaki, V., Lechner, S., Maier, F., Plattner, P., Rosenbusch, M., Wienholtz, F., Wolf, R., Nörtershäuser, W., Schweikhard, L., Malbrunot-Ettenauer, S.: First steps in the development of the multi ion reflection apparatus for collinear laser spectroscopy. Nuclear Instruments and Methods in Physics Research Section B: Beam Interactions with Materials and Atoms. https://doi.org/10.1016/j.nimb.2019.04.076, http://www.sciencedirect.com/science/article/pii/S0168583X19302605 (2019)
4. Catherall, R., Andreazza, W., Breitenfeldt, M., Dorsival, A., Focker, G.J., Gharsa, T.P., J, G.T., Grenard, J.L., Locci, F., Martins, P., Marzari, S., Schipper, J., Shornikov, A., Stora, T.: The ISOLDE facility. J. Phys. G: Nuclear Particle Phys. **44**(9), 094,002 (2017). https://doi.org/10.1088/1361-6471/aa7eba
5. Zajfman, D., Heber, O., Vejby-Christensen, L., Ben-Itzhak, I., Rappaport, M., Fishman, R., Dahan, M.: Electrostatic bottle for long-time storage of fast ion beams. Phys. Rev. A **55**, R1577–R1580 (1997). https://doi.org/10.1103/PhysRevA.55.R1577. https://link.aps.org/doi/10.1103/PhysRevA.55.R1577
6. Benner, W.H.: A gated electrostatic ion trap to repetitiously measure the charge and m/z of large electrospray ions. Anal. Chem. **69**(20), 4162–4168 (1997). https://doi.org/10.1021/ac970163e
7. Alexander, J.D., Calvert, C.R., King, R.B., Kelly, O., Bryan, W.A., Nemeth, G.R.A.J., Newell, W.R., Froud, C.A., Turcu, I.C.E., Springate, E., Orr, P.A., Pedregosa-Gutierrez, J., Walter, C.W., Williams, R.A., Williams, I.D., Greenwood, J.B.: Short pulse laser-induced dissociation of vibrationally cold, trapped molecular ions. J. Phys. B: Atomic Molec. Opt. Phys **42**(15), 154,027 (2009). https://doi.org/10.1088/0953-4075/42/15/154027
8. Lange, M., Froese, M., Menk, S., Varju, J., Bastert, R., Blaum, K., López-Urrutia, J.R.C., Fellenberger, F., Grieser, M., von Hahn, R., Heber, O., Kühnel, K.U., Laux, F., Orlov, D.A., Rappaport, M.L., Repnow, R., Schröter, C.D., Schwalm, D., Shornikov, A., Sieber, T., Toker, Y., Ullrich, J., Wolf, A., Zajfman, D.: A cryogenic electrostatic trap for long-time storage of kev ion beams. Rev. Sci. Instrum. **81**(5), 055,105 (2010). https://doi.org/10.1063/1.3372557
9. Wollnik, H., Przewloka, M.: Time-of-flight mass spectrometers with multiply reflected ion trajectories. Int. J. Mass Spectrom. Ion Processes **96**(3), 267–274 (1990). https://doi.org/10.1016/0168-1176(90)85127-N. http://www.sciencedirect.com/science/article/pii/016811769085127N
10. Plaß, W.R., Dickel, T., Czok, U., Geissel, H., Petrick, M., Reinheimer, K., Scheidenberger, C., Yavor, I.M.: Isobar separation by time-of-flight mass spectrometry for low-energy radioactive ion beam facilities. Nucl. Instrum. Methods Phys. Res. Sect. B: Beam Interact. Mater. Atoms **266**(19), 4560–4564 (2008). https://doi.org/10.1016/j.nimb.2008.05.079. http://www.sciencedirect.com/science/article/pii/S0168583X08007763. Proceedings of the XVth International Conference on Electromagnetic Isotope Separators and Techniques Related to their Applications
11. Piechaczek, A., Shchepunov, V., Carter, H., Batchelder, J., Zganjar, E., Liddick, S., Wollnik, H., Hu, Y., Griffith, B.: Development of a high resolution isobar separator for study of exotic decays. Nucl. Instrum. Methods Phys. Res. Sect/. B: Beam Interact. Mater. Atoms **266**(19), 4510–4514 (2008). https://doi.org/10.1016/j.nimb.2008.05.149. http://www.sciencedirect.com/science/article/pii/S0168583X08007660. Proceedings of the XVth International Conference on Electromagnetic Isotope Separators and Techniques Related to their Applications
12. Schury, P., Okada, K., Shchepunov, S., Sonoda, T., Takamine, A., Wada, M., Wollnik, H., Yamazaki, Y.: Multi-reflection time-of-flight mass spectrograph for short-lived radioactive ions. Europ. Phys. J. A **42**(3), 343 (2009). https://doi.org/10.1140/epja/i2009-10882-6
13. Wolf, R., Wienholtz, F., Atanasov, D., Beck, D., Blaum, K., Borgmann, C., Herfurth, F., Kowalska, M., Kreim, S., Litvinov, Y.A., Lunney, D., Manea, V., Neidherr, D., Rosenbusch, M., Schweikhard, L., Stanja, J., Zuber, K.: ISOLTRAP's multi-reflection time-of-flight mass separator/spectrometer. Int. J. Mass Spectrom. **349–350**, 123–133 (2013). https://doi.org/10.1016/j.ijms.2013.03.020. http://www.sciencedirect.com/science/article/pii/S1387380613001115. 100 years of Mass Spectrometry
14. Wienholtz, F., Beck, D., Blaum, K., Borgmann, C., Breitenfeldt, M., Cakirli, R.B., George, S., Herfurth, F., Holt, J.D., Kowalska, M., Kreim, S., Lunney, D., Manea, V., Menéndez, J., Neidherr, D., Rosenbusch, M., Schweikhard, L., Schwenk, A., Simonis, J., Stanja, J., Wolf, R.N., Zuber, K.: Masses of

exotic calcium isotopes pin down nuclear forces. Nature, 498. https://doi.org/10.1038/nature12226 (2013)
15. Beyer, T., Blaum, K., Block, M., Düllmann, C.E., Eberhardt, K., Eibach, M., Frömmgen, N., Geppert, C., Gorges, C., Grund, J., Hammen, M., Kaufmann, S., Krieger, A., Nagy, S., Nörterhäuser, W., Renisch, D., Smorra, C., Will, E.: An rfq cooler and buncher for the triga-spec experiment. Appl. Phys. B **114**(1), 129–136 (2014). https://doi.org/10.1007/s00340-013-5719-4
16. Pedersen, H.B., Strasser, D., Ring, S., Heber, O., Rappaport, M.L., Rudich, Y., Sagi, I., Zajfman, D.: Ion motion synchronization in an ion-trap resonator. Phys. Rev. Lett. **87**, 055,001 (2001). https://doi.org/10.1103/PhysRevLett.87.055001. https://link.aps.org/doi/10.1103/PhysRevLett.87.055001
17. Strasser, D., Geyer, T., Pedersen, H.B., Heber, O., Goldberg, S., Amarant, B., Diner, A., Rudich, Y., Sagi, I., Rappaport, M., Tannor, D.J., Zajfman, D.: Negative mass instability for interacting particles in a 1d box: Theory and application. Phys. Rev. Lett. **89**, 283,204 (2002). https://doi.org/10.1103/PhysRevLett.89.283204. https://link.aps.org/doi/10.1103/PhysRevLett.89.283204
18. Pedersen, H.B., Strasser, D., Amarant, B., Heber, O., Rappaport, M.L., Zajfman, D.: Diffusion and synchronization in an ion-trap resonator. Phys. Rev. A **65**, 042,704 (2002). https://doi.org/10.1103/PhysRevA.65.042704. https://link.aps.org/doi/10.1103/PhysRevA.65.042704
19. Breitenfeldt, C., Froese, M.W., Blaum, K., George, S., Grieser, M., Lange, M., Menk, S., Repnow, R., Schwalm, D., Schweikhard, L., von Hahn, R., Wolf, A.: Spreading times of ion-bunches in the cryogenic trap for fast ion beams. Int. J. Mass Spectrom. **396**, 1–4 (2016). https://doi.org/10.1016/j.ijms.2015.11.011. http://www.sciencedirect.com/science/article/pii/S1387380615004030
20. Rosenbusch, M., Kemnitz, S., Schneider, R., Schweikhard, L., Tschiersch, R., Wolf, R.N.: Towards systematic investigations of space-charge phenomena in multi-reflection ion traps. AIP Conf. Proc. **1521**(1), 53–62 (2013). https://doi.org/10.1063/1.4796061. https://aip.scitation.org/doi/abs/10.1063/1.4796061
21. Murböck, T., Schmidt, S., Andelkovic, Z., Birkl, G., Nörtershäuser, W., Vogel, M.: A compact source for bunches of singly charged atomic ions. Rev. Sci. Instrum. **87**(4), 043,302 (2016). https://doi.org/10.1063/1.4944946
22. Wolf, R.N., Marx, G., Rosenbusch, M., Schweikhard, L.: Static-mirror ion capture and time focusing for electrostatic ion-beam traps and multi-reflection time-of-flight mass analyzers by use of an in-trap potential lift. Int. J. Mass Spectrom. **313**, 8–14 (2012). https://doi.org/10.1016/j.ijms.2011.12.006. http://www.sciencedirect.com/science/article/pii/S1387380611004775
23. Bhushan, K.G., Pedersen, H.B., Altstein, N., Heber, O., Rappaport, M.L., Zajfman, D.: Radiative lifetime of the metastable $^1S_0$ state of xe^{2+}. Phys. Rev. A **62**, 012,504 (2000). https://doi.org/10.1103/PhysRevA.62.012504. https://link.aps.org/doi/10.1103/PhysRevA.62.012504
24. Saito, M., Chikaoka, A., Majima, T., Imai, M., Tsuchida, H., Haruyama, Y.: Radiative lifetime measurements of 2p3/2 and 2p1/2 metastable levels in triply charged xenon using electrostatic ion beam trap. Nucl. Instrum. Methods Phys. Res. Sect. B: Beam Interact. Mate. Atoms **414**, 68–73 (2018). https://doi.org/10.1016/j.nimb.2017.10.024. http://www.sciencedirect.com/science/article/pii/S0168583X17309436
25. Kreim, K., Bissell, M., Papuga, J., Blaum, K., Rydt, M.D., Ruiz, R.G., Goriely, S., Heylen, H., Kowalska, M., Neugart, R., Neyens, G., Nörtershäuser, W., Rajabali, M., Alarcón, R.S., Stroke, H., Yordanov, D.: Nuclear charge radii of potassium isotopes beyond n=28. Phys. Lett. B **731**, 97–102 (2014). https://doi.org/10.1016/j.physletb.2014.02.012. http://www.sciencedirect.com/science/article/pii/S0370269314001038
26. Hilger, R.T., Santini, R.E., McLuckey, S.A.: Nondestructive tandem mass spectrometry using a linear quadrupole ion trap coupled to a linear electrostatic ion trap. Analyt. Chem. **85**(10), 5226–5232 (2013). https://doi.org/10.1021/ac4007182 PMID: 23593952
27. Schury, P., Ito, Y., Wada, M., Wollnik, H.: Wide-band mass measurements with a multi-reflection time-of-flight mass spectrograph. Int. J. Mass Spectrom. **359**, 19–25 (2014). https://doi.org/10.1016/j.ijms.2013.11.005. http://www.sciencedirect.com/science/article/pii/S1387380613004053
28. Wienholtz, F., Atanasov, D., Kreim, S., Manea, V., Rosenbusch, M., Schweikhard, L., Welker, A., Wolf, R.N.: Towards ultrahigh-resolution multi-reflection time-of-flight mass spectrometry at ISOLTRAP. Physica Scripta **2015**(T166), 014,068 (2015). http://stacks.iop.org/1402-4896/2015/i=T166/a=014068
29. Dickel, T., Yavor, M.I., Lang, J., Plaß, W.R., Lippert, W., Geissel, H., Scheidenberger, C.: Dynamical time focus shift in multiple-reflection time-of-flight mass spectrometers. Int. J. Mass Spectrom. **412**, 1–7 (2017). https://doi.org/10.1016/j.ijms.2016.11.005. http://www.sciencedirect.com/science/article/pii/S1387380616302664
30. Dahl, D.A.: Simion for the personal computer in reflection. Int. J. Mass Spectrom. **200**(1), 3–25 (2000). https://doi.org/10.1016/S1387-3806(00)00305-5. http://www.sciencedirect.com/science/article/pii/S1387380600003055. Volume 200: The state of the field as we move into a new millenium

31. Maier, F.M., Fischer, P., Heylen, H., Lagaki, V., Lechner, S., Plattner, P., Sels, S., Wienholtz, F., Nörtershäuser, W., Schweikhard, L., Malbrunot-Ettenauer, S.: Simulations of a proof-of-principle experiment for collinear laser spectroscopy within a multi-reflection time-of-flight device. Hyperf. Interact. **240**(1), 54 (2019). https://doi.org/10.1007/s10751-019-1575-x
32. Appelhans, A.D., Dahl, D.A.: Simion ion optics simulations at atmospheric pressure. Int. J. Mass Spectrom. **244**(1), 1–14 (2005). https://doi.org/10.1016/j.ijms.2005.03.010. http://www.sciencedirect.com/science/article/pii/S1387380605001089
33. Manura, D., Dahl, D.: Simion 8.1 user manual. http://simion.com/ (2013)
34. Nieminen, A., Campbell, P., Billowes, J., Forest, D.H., Griffith, J.A.R., Huikari, J., Jokinen, A., Moore, I.D., Moore, R., Tungate, G., Äystö, J.: On-line ion cooling and bunching for collinear laser spectroscopy. Phys. Rev. Lett. **88**, 094,801 (2002). https://doi.org/10.1103/PhysRevLett.88.094801. https://link.aps.org/doi/10.1103/PhysRevLett.88.094801
35. Mané, E., Billowes, J., Blaum, K., Campbell, P., Cheal, B., Delahaye, P., Flanagan, K.T., Forest, D.H., Franberg, H., Geppert, C., Giles, T., Jokinen, A., Kowalska, M., Neugart, R., Neyens, G., Nörtershäuser, W., Podadera, I., Tungate, G., Vingerhoets, P., Yordanov, D.T.: An ion cooler-buncher for high-sensitivity collinear laser spectroscopy at isolde. Europ. Phys. J. **42**(3), 503–507 (2009). https://doi.org/10.1140/epja/i2009-10828-0
36. Schweikhard, L., Rosenbusch, M., Wienholtz, F., Wolf, R.N.: Isobar separation and precision mass spectrometry of short-lived nuclides with a multi-reflection time-of-flight analyzer. In: Proceedings of Science PoS (X LASNPA) 011 (2014). http://pos.sissa.it/archive/conferences/194/011/X%20LASNPA_011.pdf